Title

Collagen architecture and biomechanics of gracilis and adductor longus muscles from children with cerebral palsy

Journal

The Journal of Physiology, 602(14)

ISSN

0022-3751

Authors

Wohlgemuth, Ross P

Kulkarni, Vedant A

Villalba, Marie

et al.

Publication Date

2024-07-01

DOI

10.1113/jp285988

Peer reviewed

HHS Public Access

Author manuscript

J Physiol. Author manuscript; available in PMC 2025 February 24.

Published in final edited form as:

J Physiol. 2024 July ; 602(14): 3489–3504. doi:10.1113/JP285988.

Collagen architecture and biomechanics of gracilis and adductor longus muscles from children with cerebral palsy

Ross P. Wohlgemuth[1], **Vedant A. Kulkarni**[2], **Marie Villalba**[2], **Jon R. Davids**[2], **Lucas R. Smith**[1,3]

[1]Department of Neurobiology, Physiology, & Behavior, University of California Davis, Davis, CA, USA

[2]Department of Orthopaedic Surgery, Shriners Children's Northern California, Sacramento, CA, USA

[3]Department of Physical Medicine and Rehabilitation, University of California Davis, Davis, CA, USA

Abstract

Cerebral palsy (CP) describes some upper motoneuron disorders due to non-progressive disturbances occurring in the developing brain that cause progressive changes to muscle. While longer sarcomeres increase muscle stiffness in patients with CP compared to typically developing (TD) patients, changes in extracellular matrix (ECM) architecture can increase stiffness. Our goal was to investigate how changes in muscle and ECM architecture impact muscle stiffness, gait and joint function in CP. Gracilis and adductor longus biopsies were collected from children with CP undergoing tendon lengthening surgery for hamstring and hip adduction contractures, respectively. Gracilis biopsies were collected from TD patients undergoing anterior cruciate ligament reconstruction surgery with hamstring autograft. Muscle mechanical testing, two-photon imaging and hydroxyproline assay were performed on biopsies. Corresponding data were compared to radiographic hip displacement in CP adductors (CPA), gait kinematics in CP hamstrings (CPH), and joint range of motion in CPA and CPH. We found at matched

Corresponding author L. R. Smith: University of California, Davis, 196 Briggs Hall NPB, One Shields Ave, Davis, CA 95616-5270, USA. lucsmith@ucdavis.edu.

Author contributions

Conception and design: R.P.W., L.R.S. Data collection: R.P.W., V.A.K., M.V., J.R.D., L.R.S. Data analysis and interpretation: R.P.W., V.A.K., L.R.S. Drafting of manuscript: R.P.W., V.A.K., L.R.S.; Figure development: R.P.W., V.A.K., L.R.S. Critical revision and final approval of manuscript: R.P.W., V.A.K., M.V., J.R.D., L.R.S. All authors have read and approved the final version of this manuscript and agree to be accountable for all aspects of the work in ensuring that questions related to the accuracy or integrity of any part of the work are appropriately investigated and resolved. All persons designated as authors qualify for authorship, and all those who qualify for authorship are listed.

The peer review history is available in the Supporting Information section of this article (https://doi.org/10.1113/JP285988#support-information-section).

Competing interests

V.K. is a paid consultant for Orthopediatrics, but there is no direct relevance to the publication of this work.

Supporting information

Additional supporting information can be found online in the Supporting Information section at the end of the HTML view of the article. Supporting information files available:

Peer Review History

sarcomere lengths muscle stiffness and collagen architecture were similar between TD and CP hamstrings. However, CPH stiffness (R^2 = 0.1973), collagen content (R^2 = 0.5099) and cross-linking (R^2 = 0.3233) were correlated to decreased knee range of motion. Additionally, we observed collagen fibres within the muscle ECM increase alignment during muscular stretching. These data demonstrate that while ECM architecture is similar between TD and CP hamstrings, collagen fibres biomechanics are sensitive to muscle strain and may be altered at longer *in vivo* sarcomere lengths in CP muscle. Future studies could evaluate the impact of ECM architecture on TD and CP muscle stiffness across *in vivo* operating ranges.

Graphical Abstract

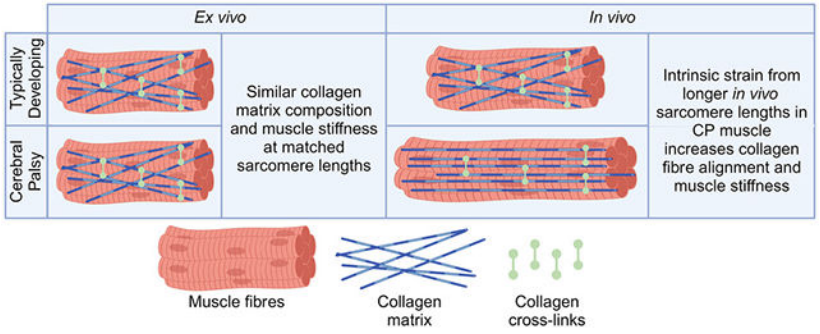

Typically developing and cerebral palsy (CP) gracilis muscles have similar extracellular matrix (ECM) composition, but longer *in vivo* sarcomere lengths in CP gracilis muscles put higher intrinsic strain on the ECM, which alters ECM architecture and increases passive stiffness.

Keywords

cerebral palsy; collagen alignment; extracellular matrix; matrix architecture; skeletal muscle

Introduction

In skeletal muscle, the organization of the myofibres and extracellular matrix (ECM) determine their active and passive mechanical functionality. The length of sarcomeres, the basic contractile unit of muscle, has a direct impact on the degree of active tension during a muscle contraction and passive tension during a passive muscular stretch (Gordon et al., 1966). In compliment to the sarcomeres, the organization of the ECM, particularly the collagenous matrix, is vital to the transmission of active tension between adjacent myofibres and from muscle to tendon (Passerieux et al., 2006, 2007), and also contributes to passive tension during a passive muscular stretch (Brashear et al., 2021; Meyer & Lieber, 2011; Ward et al., 2020). In healthy muscle the myofibres and ECM can adapt to exercise and injury by adding or repairing sarcomeres and remodelling the matrix to increase muscle strength or regenerate damaged tissue (Butterfield & Herzog, 2006; Butterfield et al., 2005; Dumont et al., 2015; Hinks et al., 2022; Kjaer, 2004; Kjaer et al., 2006; Roman et al., 2021). However, in disease there is often maladaptation in the muscle fibres and/or the ECM that results in a loss of skeletal muscle function. In cerebral palsy (CP), there is non-progressive disturbance to the developing brain that can result in muscle spasticity, gait

abnormalities and joint contractures (Crenna, 1998; Krigger, 2006; Rosenbaum et al., 2007; Sutherland & Davids, 1993). Previous reports have consistently demonstrated that spastic muscle in patients with CP operates at longer sarcomere lengths *in vivo* than non-spastic muscle (Leonard et al., 2019; Lieber & Fridén, 2002, 2019; Lieber et al., 1994; Mathewson et al., 2014, 2015; Pingel et al., 2021; Smith et al., 2011), which is implicated in reduced passive range of motion (Lieber & Fridén, 2002; Smith et al., 2011), increased muscle passive stiffness (Lieber & Fridén, 2019; Mathewson et al., 2014; Smith et al., 2011) and poor contractile strength according to the sarcomere length–tension relationship (Gordon et al., 1966). Interestingly, CP muscle bundles typically have higher passive stiffness compared to TD bundles at the same sarcomere length, without showing a difference in stiffness at the myofibre level. This is thought to be due to alterations in ECM architecture in CP muscle, specifically within the collagen matrix, that lead to changes in muscle ECM mechanics and biochemical properties.

Multiple aspects of collagen architecture, including collagen content, cross-links and alignment, change in diseased muscle and relate to muscle stiffness. Collagen content, the total collagen in the muscle, tends to increase in CP thigh muscles (Booth et al., 2001; Lieber & Fridén, 2019; Smith et al., 2011, 2021), but collagen content alone is not a consistent predictor for muscle stiffness (Lieber & Fridén, 2019; Smith et al., 2011), although it can be useful in predicting stiffness when combined with other aspects of matrix architecture (Smith et al., 2021). However, collagen cross-links, covalent bonds between collagen molecules and fibrils, are upregulated in muscle from children with CP (Smith et al., 2021) and relate to stiffness (Smith et al., 2021). Collagen cross-links also alter stretch- or strain-dependent mechanics of collagen fibrils, implying that cross-linked collagen matrices exhibit different mechanical properties depending on changes in muscle length (Depalle et al., 2015). Similarly, collagen fibre alignment, the orientation of collagen fibres within the ECM, is often increased in fibrotic muscle and relates to muscle dynamic (velocity-dependent) and elastic (velocity-independent) stiffness (Brashear et al., 2021, 2022; Sahani et al., 2022). Dynamic and elastic stiffness are relevant to the ability to stretch muscles and their static positioning, respectively, which are each affected in CP. Additionally, collagen alignment is thought to be sensitive to changes in muscle strain (Gillies et al., 2017; Purslow, 1989, 2002; Purslow & Trotter, 1994; Scarr, 2016), although this has not been quantified across a range of strains in the same muscle. Because CP muscle operates at longer *in vivo* sarcomere lengths than TD muscle, increased muscle strain in CP could activate strain-dependent biomechanical properties of collagen cross-links and collagen alignment in a way that drives CP muscle stiffness and gait kinematics *in vivo*.

Thus, the goal of this study was to compare intrinsic muscle properties of collagen architecture and tissue stiffness between TD and CP muscles, and investigate relationships between intrinsic muscle properties with clinical measures of joint mobility, three-dimensional joint kinematics and radiographic hip displacement in children with CP. We hypothesized that at matched sarcomere lengths, collagen alignment and collagen cross-linking would be increased in CP muscles compared to TD hamstrings (TDH). Further, we predicted that *in vivo* sarcomere length, collagen fibre alignment and collagen cross-linking would relate to increased stiffness in CP muscles and strongly correlate with joint mobility and kinematics. We tested this hypothesis using hamstring muscle biopsies from

TD paediatric patients, and hamstring and adductor biopsies from paediatric patients with CP. We used muscle mechanical testing to measure the passive stress and stiffness of muscle biopsies and used second harmonic generation (SHG) imaging on the biopsies to visualize collagen architecture and sarcomere length. Biopsies were then assessed for collagen content and cross-linking using the hydroxyproline and collagen solubility assays. These biomechanical and biochemical parameters were then compared to previously collected joint motion and three-dimensional joint kinematics for CP hamstring (CPH) muscles, and to joint motion and radiographic hip displacement data for CP adductor (CPA) muscles, respectively, to link intrinsic muscle properties to gait and/or joint function. This work provides new insight into the impact of muscle and ECM architecture on the joint mobility and gait patterns in children with CP.

Methods

Ethical approval

Ethical approval for this study conformed to the standards of the *Declaration of Helsinki* (except for registration in a database) and was approved by the Institutional Review Board of the Shriners Children's and WCG-IRB (tracking number 20202208; www.wcgirb.com). Since all patients were under the age of 18, informed consent was obtained from the parent(s) or legal guardian(s) of all participants prior to participation in the study. Patient data displaying age, sex, clinical outcomes and sample sizes for each assay are recorded in Table 1.

Biopsy collection and processing

For TD patients, gracilis muscle biopsies were collected during anterior cruciate ligament (ACL) reconstruction using hamstring autograft. After the gracilis muscle–tendon unit was harvested for the reconstruction, a surgical 8.0 mm clamp (Ambler Surgical, Exton, PA, USA) was used to isolate a portion of the gracilis muscle *ex vivo* at resting length for collection. For patients with CP undergoing hamstring lengthening surgery, gracilis muscle biopsies were collected *in vivo* at 90° of knee flexion and hip flexion using the same surgical clamp protocol. For patients with CP undergoing tendon lengthening surgery for hip adduction contractures, adductor longus muscle biopsies were collected *in vivo* at 90° hip flexion and 30° hip abduction (or maximum abduction if 30° was not possible) with the same surgical clamps as TDH and CPH biopsies. Since the TDH biopsy was not collected at the same joint angles as the CPH biopsy, the sarcomere length measured in the TDH was not directly compared to the CPH *in vivo* sarcomere length. Similarly, the CPA biopsy was collected at a different hip abduction angle from the CPH biopsy, so the sarcomere lengths we measured from each were not used for direct *in vivo* comparisons. For all specimens, the clamp with muscle biopsy was immediately stored in a sterilized vial of storage solution (125 mM potassium propionate, 20 mM imidazole, 5 mM EGTA, 2 mM $MgCl_2.6H_2O$, 2 mM Na_2H_2ATP in 50% glycerol; pH 7.00) (Roche et al., 2015) on ice for no more than 2 h before storage at −20°C.

Muscle mechanical testing and storage

Within 10 days of biopsy collection, muscles were tested for passive mechanical properties. Each clamped biopsy was removed from the storage solution into a room temperature bath of dissecting solution (125 mM potassium propionate, 20 mM imidazole, 5 mM EGTA, 2 mM $MgCl_2.6H_2O$, 2 mM Na_2H_2ATP; pH 7.00) (Roche et al., 2015). At least two muscle bundles were excised from the biopsy and tied at the ends with 7-0 sutures. Suture loops were attached to a 300C-LR-Dual-Mode motor arm and force transducer (Aurora Scientific, Aurora, ON Canada) in a bath of 28°C dissecting solution. Muscle bundles were mechanically tested starting either from their length within the clamp (clamp length, L_c) (TDH: $n = 8$, CPH: $n = 16$, CPA: $n = 6$) or from their slack length (length of the unloaded bundle within the dish) (TDH: $n = 7$, CPH: $n = 11$, CPA: $n = 8$).

Muscle bundles tested from *in vivo* length underwent a passive mechanical protocol that entailed a preconditioning and maintained stretch steps. The preconditioning steps took place before each maintained stretch steps and involved lengthening the muscle bundle by 5% beyond L_c at a rate of 1 Hz for 5 s. The maintained stretch steps involved stretching the muscle 5% beyond L_c at a rate of 1 L_c/s and held at the stretched length for 120 s of stress relaxation. Preconditioning and stress relaxation steps were continued up to 10%, 15% and 20% strains beyond L_c. Muscle bundles tested from slack length (L_s) underwent a passive mechanical protocol similar to bundles that were tested from *in vivo* length, except that the strains used for the slack length bundles were 7.5%, 15%, 22.5%, 30%, 37.5% and 45% strain beyond L_s. Following mechanical testing, bundles tested at L_c were fixed in 4% paraformaldehyde overnight at 4°C while bundles tested at L_s were placed in storage solution at −20°C. In some biopsies (TDH: $n = 8$, CPH: $n = 15$, CPA: $n = 10$) a small piece of tissue was removed, flash-frozen and stored at −70°C for hydroxyproline and collagen solubility assay. In biopsies that were used for bundles tested at L_s, an unexcised bundle was left in the clamp and fixed in 4% paraformaldehyde overnight at 4°C for analysis of *in vivo* sarcomere length in CP samples.

In order to directly compare the stiffness, the change in passive tension per cross-sectional area (stress) for a given change in length (strain), between samples of the two mechanical protocols, we calculated the strains that corresponded to the sarcomere length of each sample when in the clamp and reported the corresponding stiffnesses at these strains. Thus, whether a muscle bundle began its testing at initial clamped length or slack length, we normalized the stiffnesses of every sample to report the calculated stiffness at the clamped length based on the collected stress–strain data and the *in vivo* and slack sarcomere lengths measured using second harmonic generation imaging. Assuming the fibre length was equal to the muscle bundle length, we calculated the physiological cross-sectional area (PCSA) using the clamped length, L_c, mass (m), and density ($\rho = 1.06$ g/cm^3) (PCSA = m/($L_c \times \rho$)) (Mendez & Keys, 1960). Stiffness was reported as the slope of the linear fit to the plot of stress (tensile force per PCSA) and strain values. Dynamic stiffness was the slope of the linear fit with the maximum stress values during the maintained stretch steps. Dynamic stiffness represents the total increase in passive stress that occurred with each increase in strain. Elastic stiffness was the slope of the linear fit with the stress values at the end of the maintained stretch steps. Elastic stiffness represents the increase in passive stress

that was present in the muscle for a given strain following 2 min of stress relaxation. So, dynamic stiffness represents the immediate increase in passive stress on a muscle as it is stretched, while elastic stress is the increase in passive stress in muscle that remains 2 min after the stretching occurred. Elastic index or elasticity was defined as the ratio between elastic and dynamic stiffness. Elastic index values range between 0 and 1. An elastic index of 0 represents an entirely inelastic muscle which experiences complete stress-relaxation and returns to the same initial passive stress after a given stretch. An elastic index of 1 represents an entirely elastic muscle which experiences no stress-relaxation and indefinitely maintains the same increase in passive stress following a stretch. Muscles that failed before the penultimate strain in their sequence were removed from the analysis of mechanical data. These mechanical testing techniques are similar to previous studies (Brashear et al., 2021, 2022; Hakim et al., 2011; Smith & Barton, 2014; Ward et al., 2009; Wohlgemuth et al., 2023).

Second harmonic generation imaging for collagen architecture

Second harmonic generation (SHG) microscopy was performed at the Advanced Imaging Facility in the UC Davis School of Veterinary Medicine using a Leica TCS SP8 (Leica Microsystems Inc. Deerfield, IL, USA) fit with a Mai Tai deep see laser (Spectra-Physics, Milpitas, CA, USA). A ×25 water immersion objective was used in conjunction with a multiphoton laser. SHG imaging was done on muscle bundles fixed in 4% paraformaldehyde overnight (TDH: $n = 9$, CPH: $n = 19$, CPA: $n = 7$) and bundles kept in storage solution (TDH: $n = 6$, CPH: $n = 8$, CPA: $n = 7$) within 1 week following mechanical testing. Fixed muscle bundles were imaged three times in random locations using the multiphoton laser tuned to 870 nm and 830 nm in series. Since the achievable depth of SHG imaging in skeletal muscle is approximately 100 μm (Plotnikov et al., 2006), in each of the three imaged locations, image stacks were obtained with a thickness of 100 μm and slice thickness of 1 μm. This imaging technique is similar to previous studies (Brashear et al., 2021, 2022). Muscle bundles stored in storage solution were imaged in one location across a range of strains from slack length to 145% of L_s in line with the mechanical protocol. Unfixed muscle bundles were imaged using a multiphoton laser tuned to 848 nm for an image stack size of at least 50 μm with a slice thickness of 1 μm. Custom MATLAB (MathWorks, Natick, MA, USA) scripts and processing in ImageJ (NIH, Bethesda, MD, USA) were used to analyse the image stacks as previously described (Brashear et al., 2021, 2022; Hu et al., 2021).

Hydroxyproline and collagen solubility assay

Collagen content and cross-linking were quantified in muscle biopsies using the hydroxyproline and collagen solubility assay similar to other studies (Flesch et al., 1997; Heydemann et al., 2005; Smith & Barton, 2014) and as described previously (Brashear et al., 2021, 2022; Wohlgemuth et al., 2023). Flash-frozen muscle samples were powdered using mortar and pestle that were cooled on dry ice. The mass of powdered samples was recorded, and each sample was placed in 1 ml of phosphate buffered saline (PBS) and shaken for 30 min at 4°C. Samples were then centrifuged at 21,000 *g* for 30 min at 4°C. The supernatant was discarded and the pellet was placed in a 1:10 (w/v) solution of 0.5 M acetic acid with 1 mg/ml pepsin to stir overnight at 4°C. The following day the samples were centrifuged

for 30 min at 21,000 *g* at 4°C and separated into the supernatant (soluble fraction) and pellet (insoluble fraction). The supernatant was boiled off and then 0.5 M HCl was added to each supernatant and pellet as well as to an array of standards with known hydroxyproline concentrations. All samples and standards were boiled in closed tubes overnight. The next day each sample was vortexed and 10 µl was aliquoted into a separate tube for the final steps. A combination of 150 µl of isopropanol and 75 µl of Solution A (1:4 dilution of 7% chloramine T to acetate citrate buffer) was added to each tube before mixing and leaving at room temperature for 10 min. One millilitre of Solution B (3:13 dilution of Erlich's reagent to isopropanol) was added to each tube before mixing and placing on a 58°C hot plate for 30 min. Following the incubation period, samples were removed from the hot plate and put on ice before centrifuging at 5000 *g* for 1 min at 4°C. The supernatants of each sample were plated in duplicate, and absorbance was measured at 558 nm. Total collagen and cross-linking were back-calculated using the standard absorbance curve and data were reported as µg collagen per mg powdered tissue and percentage of insoluble collagen.

Clinical data and gait analysis

For children with CP undergoing hamstring lengthening surgery, popliteal angles were measured intra-operatively and were defined as the angle of the lower leg relative to vertical during passive knee extension with the hip flexed at 90° (Fig. 1). For children with CP undergoing hip tendon lengthening, hip abduction angle was measured intra-operatively with the sacrum positioned flat on the operating room table and hips flexed to 90°, with each hip's abduction angle measured as the angle between the thigh relative to vertical (Fig. 1). Hip migration percentage (MP), the most important radiographic measure of clinical hip displacement, was calculated from a supine anterior–posterior pelvis radiograph. MP = $A/B \times 100\%$, where A is distance between the lateral edge of the acetabulum to the lateral edge of the femoral head and B is the width of the femoral head (Fig. 1).

Three-dimensional gait analysis was performed on patients with CPH contractures with a GMFCS score of 1–3. Motion capture data were collected at 120 Hz using 12 motion capture cameras (Motion Analysis Corporation, Rohnert Park, CA, USA). A clinician attached 24 reflective markers to the surface of patients' skin using double-sided tape, following the full-body Plug-in Gait model (McMulkin & Gordon, 2009; Wren et al., 2008). Hip joint centres were approximated from the locations of the anterior superior iliac spines using regression equations. Knee joint centres were approximated as the midpoint between lateral and medial femoral condyle locations. Ankle joint centres were approximated as the midpoint between lateral and medial malleolus locations. After collecting a static calibration trial, patients walked back and forth across the lab at a self-selected pace while kinematic data were collected. Joint angles were calculated using a Cardan $x–y–z$ rotation sequence corresponding to flexion/extension, varus/valgus, and internal/external rotation. Discrete values of knee flexion angles at initial contact, peak knee flexion and extension in stance and swing, range of knee flexion/extension motion, and average knee flexion in stance and swing were calculated and stored for further analysis. A previously collected data set of gait analysis data performed on TD patients was used to compare to our data set on patients with CPH contractures.

Statistical methods

Statistics were performed in GraphPad Prism (GraphPad Software, Boston, MA, USA). An *a priori* power analysis based on a previous study (Smith et al., 2011) predicted an effect size of 0.93 between TD and CP muscle bundle elastic stiffness (TD: ~25 ± 11 kPa/μm; CP: ~40 ± 20 kPa/μm). Based on this power analysis we planned to collect a minimum of 40 samples between TD and CP gracilis biopsies to achieve 80% power. One-way ANOVA was performed to compare muscle mechanics, sarcomere length and collagen architecture across muscle groups (TDH, CPH and CPA). Two-way ANOVA was used to compare muscle mechanics and collagen architecture across muscle groups and muscle strain (degree of stretch). For both one-way and two-way ANOVAs, a *post hoc* Dunnett's or Tukey's multiple comparisons test was used to find specific differences between groups. Student's unpaired *t* test was used to compare clinical and functional parameters between CPH and CPA groups. Simple linear regressions were used to compare continuous variables from the muscle mechanics, sarcomere length, collagen architecture and clinical/functional datasets. Significance was set at $P < 0.05$. Unless otherwise stated, data are reported as means ± SD.

Results

Passive mechanics and muscle architecture

Although fixed muscle contractures in CP are excessively stiff, surprisingly, muscle bundles that were excised from biopsies for mechanical testing (Fig. 2A) were not significantly different in mass, length or physiological cross-sectional area between groups (Fig. 3A-C). There was a significant effect of muscle group ($P = 0.0065$) on clamped sarcomere length (Fig. 2B), such that clamped sarcomere lengths of CPH and CPA muscle bundles were 13.1% and 25.0% longer, respectively, than TDH bundles. Dynamic and elastic stress significantly increased with strain (Dynamic: $P < 0.0001$; Elastic: $P < 0.0001$) and there was a significant interaction between strain and muscle group (Dynamic: $P = 0.0070$; Elastic: $P = 0.0004$), such that CPA muscle bundles had a greater increase in dynamic and elastic stress over the range of strains than TDH and CPH bundles (Fig. 2C and D). However, there were no differences in dynamic or elastic stiffness between muscles (Fig. 2E and F). Elastic index represented the level of relative elasticity on a scale of 0 (not elastic) to 1 (completely elastic) during muscle mechanical testing. Elastic index was 20.4% higher in CPA muscle bundles compared to CPH ($P = 0.0033$), but there was no difference in elastic index between TDH and CPH bundles (Fig. 2G). Overall, CPA muscle bundles had a greater elasticity and a steeper stress–strain curve than CPH and TDH bundles.

Collagen fibre architecture, content and cross-linking

Collagen architecture has been correlated to muscle stiffness (Brashear et al., 2021, 2022; Sahani et al., 2022) and thus was investigated in the muscle biopsies. Alignment index, a value ranging between 0 (perfect unalignment) to 1 (perfect alignment), was used to measure collagen fibre alignment in muscle bundles (Fig. 4A). In muscle bundles that were imaged across a range of strains, alignment index demonstrated the dynamic changes in alignment that occur over the series of images (Fig. 4A). Collagen fibre alignment at clamped sarcomere length did not significantly vary between muscle groups (Fig. 4B). However, collagen fibre alignment increased with increasing muscle strain in all muscles

tested ($P < 0.0001$) (Fig. 4C). Collagen alignment index was not significantly correlated with dynamic stiffness (Fig. 4D), but there was a significant correlation between alignment index and elastic index overall ($P = 0.0064$, $R^2 = 0.1318$) and within CPA muscles ($P = 0.0169$, $R^2 = 0.3906$) (Fig. 4E).

Biochemical measures of collagen content and cross-linking have shown relationships to stiffness in some muscles from patients with CP; however, in our study collagen content and cross-linking, measured by the hydroxyproline and collagen solubility assay, were not significantly different between muscle groups (Fig. 5A and B). There was a positive correlation between total collagen and elastic stiffness across all muscles ($P = 0.0180$, $R^2 = 0.1728$) (Fig. 5C), as well as between insoluble (cross-linked) collagen and elastic stiffness across all muscles ($P = 0.0167$, $R^2 = 0.1763$) (Fig. 5D). There were negative correlations between total collagen and insoluble collagen compared to elastic index in the TDH muscles (Total collagen: $P = 0.0195$, $R^2 = 0.6248$; Insoluble collagen: $P = 0.0189$, $R^2 = 0.6284$) (Fig. 5E and F). Taken altogether, there were no evident differences in ECM content or architecture between the muscle groups, but the collagen fibres in all muscles showed dynamic re-alignment upon muscle stretching.

Relationships between muscle parameters and clinical assessment of patients with cerebral palsy

Because muscle contractures limit joint range of motion and alter gait patterns, an array of parameters related to joint mobility and spasticity were collected using clinical measurements of knee and hip joints (Fig. 6B) and a 3-D gait analysis program. When comparing CPA muscles grouped by GMFCS 1–3 and GMFCS 4–5, there was a trend for 35% higher hip migration percentage in GMFCS 4–5 patients compared to 1–3 patients ($P = 0.1278$) (Fig. 6A). However, there was no significant difference in popliteal angle between GMFCS 1–3 and 4–5 groups in CPH muscles (Fig. 6A). Using previously collected gait data from TD patients, we plotted different measures of gait function with a specific focus on knee flexion between the previous data set averages and patients with CPH contractures (Fig. 6C and D). These plots display that while cadence is not different between TD and CPH groups, there was a 22.0% decrease in walking speed in the CPH group ($P < 0.0001$) and highly significant ($P < 0.0001$) increases in knee flexion in stance phase (21.57° increase in CPH), swing phase (14.57° increase in CPH), initial contact (IC) (35.53° increase in CPH) and overall (18.58° increase in CPH) (Fig. 6C and D). These increases in knee flexion reflect the effects of hamstring contractures reducing the range of motion on the knee joint during ambulation. We compared these clinical measures and gait parameters to our dataset of muscle mechanics, sarcomere length and collagen architecture. We found that total collagen ($P = 0.0041$, $R^2 = 0.5099$), insoluble collagen ($P = 0.0339$, $R^2 = 0.3233$) and elastic stiffness ($P = 0.0261$, $R^2 = 0.1973$) were all predictive of increased popliteal angle in CPH muscles (Fig. 6E-G). We also found that a higher hip migration percentage was negatively associated with collagen alignment index ($P = 0.0146$, $R^2 = 0.4035$) (Fig. 6H). Related to the gait parameters, we found that sarcomere length was actually negatively correlated to the mean knee flexion in the stance phase ($P = 0.0131$, $R^2 = 0.3880$) and across the entire gait cycle ($P = 0.0156$, $R^2 = 0.3731$), contrary to our expectations (Fig. 6I, J).

Overall, we found that collagen architecture and sarcomere length relate to joint motion and gait function in patients with CP.

Discussion

The goal of this study was to compare muscle stiffness and collagen architecture between TDH and CP muscles and assess if intrinsic properties of muscle tissue relate to functional measures of joint mobility, gait kinematics and radiographic structure in children with CP. Unexpectedly, we found that there were no significant differences in collagen architecture or passive stiffness between CPH and TDH muscles at matched sarcomere lengths. However, we demonstrated that collagen content, collagen alignment and *in vivo* sarcomere length correlated to joint function and gait kinematics in children with CP. Further, we provided evidence that the structure of the collagen matrix within the gracilis drives passive stiffness, which in turn affects the range of motion at the knee joint. Therefore, while there were few differences detected in the *ex vivo* collagen architecture and mechanical properties between TDH and CP muscles, the differences in intrinsic strain between TDH and CP muscles *in vivo* could lead to differences in collagen architecture and mechanical properties across the *in vivo* joint range of motion.

Muscle passive mechanical properties depend on the structural makeup of the tissue and the relative strain on the muscle. While there were not differences in collagen architecture and muscle stiffness at matched sarcomere lengths between CP and TDH muscles, since CP muscles operate at longer sarcomere lengths *in vivo*, they have higher intrinsic strain on the muscle and increased *in vivo* mechanical properties compared to TD muscles (Leonard et al., 2019; Lieber & Fridén, 2002, 2019; Lieber et al., 1994; Mathewson et al., 2014, 2015; Pingel et al., 2021; Smith et al., 2011). Placing increased strain on structural components in the muscle fibres and ECM alters their passive mechanical behaviour. This is exemplified by viscoelastic proteins titin and collagen, which both exhibit non-linear passive mechanical behaviour in response to changes in muscle strain (Depalle et al., 2015; Freundt & Linke, 2019; Prado et al., 2005; Ward et al., 2020). Although previous reports show little to no changes in titin content and isoform size, there is evidence that collagen content and cross-linking are altered in some CP muscles compared to TD controls (Lieber & Fridén, 2019; Smith et al., 2011, 2012, 2021). Nevertheless, because CP muscle operates at a higher intrinsic muscle strain (longer *in vivo* sarcomere lengths) than TD muscle, the length sensitive ECM architecture will be altered in CP muscle *in vivo*. This elongated ECM would contribute to the high tissue stiffness found in contracture. Essentially, when *in vivo* the same collagen matrix in the CP muscle is strained across a range of longer sarcomere lengths than in the TD muscle, which results in a different degree of passive mechanical contribution from the CP collagen matrix than the TD collagen matrix. Further, because the ECM will exert different mechanical properties depending on the *in vivo* operating range, the same amount of collagen cross-links in a CPH could be related to a higher popliteal angle whereas in the TDH they are not related to any change in knee range of motion. Importantly, the *in vivo* operating range of a muscle changes the effect its structural makeup has on its mechanical function. Future studies could expand on this concept by performing mechanical testing and measurements of dynamic collagen architecture relative to *in vivo* sarcomere length of TD and CP muscles.

Our results show that the collagen content and cross-linking in TDH and CPH muscles are largely similar. Collagen content is altered in CP on a muscle-specific basis, such that there are increases in some CP muscles, such as the gracilis, semitendinosus (Lieber & Fridén, 2019; Smith et al., 2011, 2021) and vastus lateralis (Booth et al., 2001), but not in others such as the soleus and gastrocnemius (Lieber & Fridén, 2019; Mathewson et al., 2014). Even though we did not observe a change in collagen content in the CP gracilis muscles compared to TD, this is not contradictory to a previous study that showed that CP gracilis collagen only trended to be higher than TD gracilis, and was not significantly different (Smith et al., 2011). While we did not present a TD control for the CP adductor longus, our study provides new data that show collagen content is similar between CP gracilis and adductor longus muscles. In contrast to collagen content, collagen cross-linking has only been measured in CP muscles in one study (Smith et al., 2021), although a transcriptional study showed an increase in cross-linking enzyme expression in CP hamstring muscles (Smith et al., 2012). Even though CP muscle ECM structure was highly similar to TDH controls, collagen content and cross-links were positively correlated to elastic stiffness across all muscles; however, neither total nor cross-linked collagen was significantly correlated to stiffness within TDH, CPH, or CPA. This finding is aligned with studies that have shown collagen content alone is not a consistent predictor for muscle stiffness within CP muscles (Lieber & Fridén, 2019; Mathewson et al., 2014; Smith et al., 2011). Taken altogether, the amount of collagen and cross-links were not strong predictors of passive muscle stiffness in our study.

Collagen alignment has been implicated in muscle stiffness and is increased in the dystrophic muscle ECM (Brashear et al., 2021, 2022; Sahani et al., 2022). Additionally, previous studies have predicted that the alignment of collagen fibres dynamically changes during a muscle shortening or lengthening (Gillies et al., 2017; Purslow, 1989, 2002; Purslow & Trotter, 1994; Scarr, 2016).While we did not observe differences in collagen alignment between TDH and CP muscles, we provided a novel visualization and quantification of strain-dependent dynamic re-alignment of collagen fibres in human muscle. Even so, we did not observe a significant relationship between collagen alignment and passive muscle mechanics over the range of strains tested. Notably, our study measured dynamic collagen alignment within muscle bundles starting at slack length and up to 45% strain beyond slack length; while this range of strains was effective in visualizing and quantifying the strain-dependent increase in collagen alignment, this study could have been improved by measuring collagen alignment over a range of sarcomere lengths instead of a range of strains relative to clamped muscle length. Further, one limitation of our study was the separation of mechanical testing and SHG imaging. By combining concurrent mechanical testing and SHG imaging, direct comparisons between collagen alignment and mechanical stiffness would provide greater power compared to measuring the two parameters separately. It is possible that in CP muscle longer sarcomere lengths *in vivo* could lead to increased collagen alignment compared to TD muscle. Increased *in vivo* collagen alignment would affect the dynamics of collagen fibre re-alignment during a muscle stretch since highly aligned collagen would be less able to deform to accommodate increases in passive loading along the muscle tissue. Upon loading the collagen matrix, collagen fibres first re-align, straighten, and then undergo molecular sliding and stretching of the backbone with increasing load (Depalle et al., 2015; Purslow, 1989; Purslow &

Trotter, 1994). If collagen fibres started highly aligned within the *in vivo* operating range of motion, further strain on the muscle could result in increased collagen molecular sliding instead of changes in alignment, which would correspond to higher passive tension and stiffness according to typical mechanical behaviour of collagen fibrils (Depalle et al., 2015). Increased passive tension and alignment of collagen fibrils could contribute to increased resistance of collagen fibres to enzymatic degradation (Saini et al., 2020) and the mechanosensitive actions of satellite cells and fibro-adipogenic progenitors within muscle (Hu et al., 2021; Loomis & Smith, 2023; Loomis et al., 2022). For these reasons, the intrinsic strain imposed on CP muscle via longer *in vivo* sarcomere lengths could have large impacts on collagen architecture and biomechanics that were not observed in our *ex vivo* muscle biopsy mechanical and visual experiments.

Somewhat paradoxically, although there were not significant differences in muscle stiffness, collagen content, or collagen alignment between TDH and CP muscles at matched sarcomere lengths, we still observed significant relationships between intrinsic muscle properties and *in vivo* knee and hip joint clinical measures. Knee joint motion measured by the popliteal angle was assessed under anaesthesia, capturing myostatic contracture, which depends on intrinsic muscle biomechanics, rather than spasticity or voluntary contraction, which depends on neuronal input. Although there are multiple muscles controlling the flexion range of motion at the knee, we demonstrate that the passive stiffness of the gracilis is related to reduced range of flexion on three-dimensional gait kinematics. When integrating collagen content and cross-linking, we observe that the amounts of total and cross-linked collagen relate to muscle stiffness across groups and also to popliteal angle in children with CPH contractures. Although total and insoluble collagen were not directly related to CPH stiffness, but rather stiffness across all muscles tested, this study provides evidence that the contents and architecture of the muscle collagen matrix contribute to the mechanical properties of the muscle and range of motion at the corresponding joint. Future studies should integrate more aspects of ECM architecture to determine which other material properties of the matrix relate to CP muscle stiffness and joint range of motion. In contrast, the CPA muscles do not show integrative relationships between the collagen matrix, muscle stiffness and clinical outcomes. We did observe that a lower degree of collagen fibre alignment was related to a higher degree of hip migration percentage, which clinically correlates to a higher risk of subsequent displacement, dislocation and development of pain (Soo et al., 2006). This link is harder to explain given the evidence that higher collagen alignment is usually correlated to increased muscle stiffness, decreased collagen degradability and poor functional outcomes. Further study is needed to reveal how a lower degree of collagen alignment is detrimental to CP adductor function. Another point of further study is the relationship between *in vivo* sarcomere length and the degree of knee flexion during the gait cycle. We observed a negative correlation between sarcomere length and knee flexion across the gait cycle and in the stance phase. These findings suggest that muscles with a higher *in vivo* sarcomere length have decreased flexion during gait and specifically in stance phase. While longer sarcomere lengths in TDH would be indicative of less knee flexion, CPH muscles in contracture have longer *in vivo* sarcomere lengths (Leonard et al., 2019; Lieber & Fridén, 2002, 2019; Lieber et al., 1994; Mathewson et al., 2014, 2015; Pingel et al., 2021; Smith et al., 2011) and are more flexed during gait. This

discrepancy could be further researched with the development of novel imaging modalities that enable measurement of sarcomere length across a muscle's range of motion (Adkins et al., 2021; Pincheira et al., 2022; Sanchez et al., 2015; Young et al., 2017).

Finally, we acknowledge some limitations of our study. We realize that our measured *in vivo* sarcomere lengths for CP gracilis muscles were shorter than observed in other studies (Lieber & Fridén, 2019; Smith et al., 2011). This could have been due to a difference in methods, where we used SHG microscopy to measure sarcomere length at the surface of the muscle bundles while typically laser diffraction is used to measure sarcomere length throughout the entire biopsy. Future studies could investigate the differences in SL measurements between SHG microscopy and laser diffraction. Additionally, the mean age of the TD population in our study was higher than the CP population, which could contribute to changes in muscle properties. While we did find a minorly significant correlation between age and elastic stiffness in the TDH group ($P = 0.0428$, $R^2 = 0.2793$), we did not observe any other significant correlations between age and muscle mechanics or collagen architecture. Our age ranges within the TD and CP study populations also reflect inherent age differences at which ACL reconstruction and tendon lengthening surgeries are performed.

Overall, we found that the mechanical properties and ECM architecture of the CPH and TDH muscles were comparable at matched sarcomere lengths, but aspects of ECM architecture were still useful in predicting *in vivo* knee joint range of motion in children with CP. Also, we demonstrated that the alignment of collagen fibres within TDH and CP muscles is robustly dynamic upon muscle stretching. From our data we infer that longer *in vivo* sarcomeres in CP muscle increase the intrinsic strain on muscle ECM components that drive changes in muscle mechanics that are difficult to observe *ex vivo*. We suggest future studies should further investigate how ECM architecture and biomechanics are affected by operating at longer *in vivo* sarcomere lengths in CP muscle compared to TD muscle.

Supplementary Material

Refer to Web version on PubMed Central for supplementary material.

Acknowledgements

The authors appreciate the Gait Lab at Shriners Children's Northern California, especially Patrick Fischer, for collecting the gait data and providing consultation on the analysis of gait parameters in this study. The authors acknowledge and appreciate the participation of Amanda Whitaker, MD; Nicole Friel, MD, MS; Brian Haus, MD; from Shriners Children's Northern California in providing tissue samples for this study. The authors would like to thank the Health Sciences District Advanced Imaging Facility and Ingrid Brust-Mascher for providing access to the two-photon microscope. The authors would like to thank current and former members of the MyoMatrix Lab including Taryn Loomis, Madison Stewart, Sarah Brashear, Perri Gish, Lin-ya Hu, Ryan Feitzinger, Daryl Dinh, Sathvik Sriram, and Kyle Henricson for insightful conversations and thoughtful review of the data. The authors would also like to thank Mr Harlan Zimmerman whose generously supported initiation of this work. Finally, the authors are also grateful to the patients at Shriners Children's Northern California for making this study possible.

Funding

This work was supported by a grant from the Hartwell Foundation. This work is made possible by the generosity of Mr Harlan Zimmerman.

Biography

Ross P. Wohlgemuth graduated from Cal Poly San Luis Obispo in 2019 with a BS in Biological Sciences and a minor in Mathematics. He joined Lucas Smith's lab at UC Davis in 2020 as a PhD student in the Molecular, Cellular, & Integrative Physiology graduate group. He has a keen interest in the connection between collagen fibre architecture and biomechanics in healthy and diseased skeletal muscle. After finishing his PhD he plans to continue studying the muscle extracellular matrix as a postdoc and eventually as a professor.

Data availability statement

The data the support the findings of this study will be made upon reasonable request.

References

Adkins AN, Dewald JPA, Garmirian LP, Nelson CM, & Murray WM (2021). Serial sarcomere number is substantially decreased within the paretic biceps brachii in individuals with chronic hemiparetic stroke. Proceedings of the National Academy of Sciences, USA, 118(26), e2008597118.

Booth CM, Cortina-Borja MJ, & Theologis TN (2001). Collagen accumulation in muscles of children with cerebral palsy and correlation with severity of spasticity. Developmental Medicine and Child Neurology, 43(5), 314–320. [PubMed: 11368484]

Brashear SE, Wohlgemuth RP, Gonzalez G, & Smith LR (2021). Passive stiffness of fibrotic skeletal muscle in mdx mice relates to collagen architecture. The Journal of Physiology, 599(3), 943–962. [PubMed: 33247944]

Brashear SE, Wohlgemuth RP, Hu L-YR, Jbeily EH, Christiansen BA, & Smith LR (2022). Collagen cross-links scale with passive stiffness in dystrophic mouse muscles, but are not altered with administration of lysyl oxidase inhibitor. PLoS ONE, 17(10), e0271776. [PubMed: 36302059]

Butterfield TA, & Herzog W (2006). The magnitude of muscle strain does not influence serial sarcomere number adaptations following eccentric exercise. Pflugers Archiv: European Journal of Physiology, 451(5), 688–700. [PubMed: 16133258]

Butterfield TA, Leonard TR, & Herzog W (2005). Differential serial sarcomere number adaptations in knee extensor muscles of rats is contraction type dependent. Journal of Applied Physiology, 99(4), 1352–1358. [PubMed: 15947030]

Crenna P. (1998). Spasticity and "spastic" gait in children with cerebral palsy. Neuroscience and Biobehavioral Reviews, 22(4), 571–578. [PubMed: 9595571]

Depalle B, Qin Z, Shefelbine SJ, & Buehler MJ (2015). Influence of cross-link structure, density and mechanical properties in the mesoscale deformation mechanisms of collagen fibrils. Journal of the Mechanical Behavior of Biomedical Materials, 52, 1–13. [PubMed: 25153614]

Dumont NA, Bentzinger CF, Sincennes MC, & Rudnicki MA (2015). Satellite cells and skeletal muscle regeneration. Comprehensive Physiology, 5(3), 1027–1059. [PubMed: 26140708]

Flesch M, Schiffer F, Zolk O, Pinto Y, Rosenkranz S, Hirth-Dietrich C, Arnold G, Paul M, & Bohm M (1997). Contractile systolic and diastolic dysfunction in renin-induced hypertensive cardiomyopathy. Hypertension, 30(3 Pt 1), 383–391. [PubMed: 9314421]

Freundt JK, & Linke WA (2019). Titin as a force-generating muscle protein under regulatory control. Journal of Applied Physiology, 126(5), 1474–1482. [PubMed: 30521425]

Gillies AR, Chapman MA, Bushong EA, Deerinck TJ, Ellisman MH, & Lieber RL (2017). High resolution three-dimensional reconstruction of fibrotic skeletal muscle extracellular matrix. The Journal of Physiology, 595(4), 1159–1171. [PubMed: 27859324]

Gordon AM, Huxley AF, & Julian FJ (1966). The variation in isometric tension with sarcomere length in vertebrate muscle fibres. The Journal of Physiology, 184(1), 170–192. [PubMed: 5921536]

Hakim CH, Grange RW, & Duan D (2011). The passive mechanical properties of the extensor digitorum longus muscle are compromised in 2-to 20-mo-old mdx mice. Journal of Applied Physiology, 110(6), 1656–1663. [PubMed: 21415170]

Heydemann A, Huber JM, Demonbreun A, Hadhazy M, & McNally EM (2005). Genetic background influences muscular dystrophy. Neuromuscular Disorders, 15(9-10), 601–609. [PubMed: 16084087]

Hinks A, Jacob K, Mashouri P, Medak KD, Franchi MV, Wright DC, Brown SHM, & Power GA (2022). Influence of weighted downhill running training on serial sarcomere number and work loop performance in the rat soleus. Biology Open, 11(7), bio059491. [PubMed: 35876382]

Hu LY, Mileti CJ, Loomis T, Brashear SE, Ahmad S, Chellakudam RR, Wohlgemuth RP, Gionet-Gonzales MA, Leach JK, & Smith LR (2021). Skeletal muscle progenitors are sensitive to collagen architectural features of fibril size and cross linking. American Journal of Physiology-Cell Physiology, 321(2), C330–C342. [PubMed: 34191625]

Kjaer M. (2004). Role of extracellular matrix in adaptation of tendon and skeletal muscle to mechanical loading. Physiological Reviews, 84(2), 649–698. [PubMed: 15044685]

Kjaer M, Magnusson P, Krogsgaard M, Møller JB, Olesen J, Heinemeier K, Hansen M, Haraldsson B, Koskinen S, Esmarck B, & Langberg H (2006). Extracellular matrix adaptation of tendon and skeletal muscle to exercise. Journal of Anatomy, 208(4), 445–450. [PubMed: 16637870]

Krigger KW (2006). Cerebral palsy: An overview. American Family Physician, 73(1), 91–100. [PubMed: 16417071]

Leonard TR, Howard JJ, Larkin-Kaiser K, Joumaa V, Logan K, Orlik B, El-Hawary R, Gauthier L, & Herzog W (2019). Stiffness of hip adductor myofibrils is decreased in children with spastic cerebral palsy. Journal of Biomechanics, 87, 100–106. [PubMed: 30853092]

Lieber RL, & Fridén J (2002). Spasticity causes a fundamental rearrangement of muscle-joint interaction. Muscle & Nerve, 25(2), 265–270. [PubMed: 11870696]

Lieber RL, & Fridén J (2019). Muscle contracture and passive mechanics in cerebral palsy. Journal of Applied Physiology, 126(5), 1492–1501. [PubMed: 30571285]

Lieber RL, Loren GJ, & Fridén J (1994). In vivo measurement of human wrist extensor muscle sarcomere length changes. Journal of Neurophysiology, 71(3), 874–881. [PubMed: 8201427]

Loomis T, Hu L-Y, Wohlgemuth RP, Chellakudam RR, Muralidharan PD, & Smith LR (2022). Matrix stiffness and architecture drive fibro-adipogenic progenitors' activation into myofibroblasts. Scientific Reports, 12(1), 13582. [PubMed: 35945422]

Loomis T, & Smith LR (2023). Thrown for a loop: Fibro-Adipogenic progenitors in skeletal muscle fibrosis. American Journal of Physiology-Cell Physiology, 325(4), C895–C906. [PubMed: 37602412]

Mathewson MA, Chambers HG, Girard PJ, Tenenhaus M, Schwartz AK, & Lieber RL (2014). Stiff muscle fibers in calf muscles of patients with cerebral palsy lead to high passive muscle stiffness. Journal of Orthopaedic Research, 32(12), 1667–1674. [PubMed: 25138654]

Mathewson MA, Ward SR, Chambers HG, & Lieber RL (2015). High resolution muscle measurements provide insights into equinus contractures in patients with cerebral palsy. Journal of Orthopaedic Research, 33(1), 33–39. [PubMed: 25242618]

McMulkin ML, & Gordon AB (2009). The effect of static standing posture on dynamic walking kinematics: Comparison of a thigh wand versus a patella marker. Gait & Posture, 30(3), 375–378. [PubMed: 19631547]

Mendez J, & Keys A (1960). Density and composition of mammalian muscle. Metabolism, 9(2), 184–188.

Meyer GA, & Lieber RL (2011). Elucidation of extracellular matrix mechanics from muscle fibers and fiber bundles. Journal of Biomechanics, 44(4), 771–773. [PubMed: 21092966]

Passerieux E, Rossignol R, Chopard A, Carnino A, Marini JF, Letellier T, & Delage JP (2006). Structural organization of the perimysium in bovine skeletal muscle: Junctional plates and associated intracellular subdomains. Journal of Structural Biology, 154(2), 206–216. [PubMed: 16503167]

Passerieux E, Rossignol R, Letellier T, & Delage JP (2007). Physical continuity of the perimysium from myofibers to tendons: involvement in lateral force transmission in skeletal muscle. Journal of Structural Biology, 159(1), 19–28. [PubMed: 17433715]

Pincheira PA, Boswell MA, Franchi MV, Delp SL, & Lichtwark GA (2022). Biceps femoris long head sarcomere and fascicle length adaptations after 3 weeks of eccentric exercise training. Journal of Sport and Health Science, 11(1), 43–49. [PubMed: 34509714]

Pingel J, Kampmann M-L, Andersen JD, Wong C, Døssing S, Børsting C, & Nielsen JB (2021). Gene expressions in cerebral palsy subjects reveal structural and functional changes in the gastrocnemius muscle that are closely associated with passive muscle stiffness. Cell and Tissue Research, 384(2), 513–526. [PubMed: 33515289]

Plotnikov S, Juneja V, Isaacson AB, Mohler WA, & Campagnola PJ (2006). Optical clearing for improved contrast in second harmonic generation imaging of skeletal muscle. Biophysical Journal, 90(1), 328–339. [PubMed: 16214853]

Prado LG, Makarenko I, Andresen C, Krüger M, Opitz CA, & Linke WA (2005). Isoform diversity of giant proteins in relation to passive and active contractile properties of rabbit skeletal muscles. Journal of General Physiology, 126(5), 461–480. [PubMed: 16230467]

Purslow PP (1989). Strain-induced reorientation of an intra-muscular connective tissue network: Implications for passive muscle elasticity. Journal of Biomechanics, 22(1), 21–31. [PubMed: 2914969]

Purslow PP (2002). The structure and functional significance of variations in the connective tissue within muscle. Comparative Biochemistry and Physiology-Part A, Molecular & Integrative Physiology, 133(4), 947–966.

Purslow PP, & Trotter JA (1994). The morphology and mechanical properties endomysium in series-fibred muscles: Variations with muscle length. Journal of Muscle Research and Cell Motility, 15(3), 299–308. [PubMed: 7929795]

Roche SM, Gumucio JP, Brooks SV, Mendias CL, & Claflin DR (2015). Measurement of maximum isometric force generated by permeabilized skeletal muscle fibers. Journal of Visualized Experiments, 2015(100), e52695.

Roman W, Pinheiro H, Pimentel MR, Segalés J, Oliveira LM, García-Domínguez E, Gómez-Cabrera MC, Serrano AL, Gomes ER, & Muñoz-Cánoves P (2021). Muscle repair after physiological damage relies on nuclear migration for cellular reconstruction. Science, 374(6565), 355–359. [PubMed: 34648328]

Rosenbaum P, Paneth N, Leviton A, Goldstein M, Bax M, Damiano D, Dan B, & Jacobsson B (2007). A report: The definition and classification of cerebral palsy April 2006. Developmental Medicine and Child Neurology Supplement, 109, 8–14. [PubMed: 17370477]

Sahani R, Wallace CH, Jones BK, & Blemker SS (2022). Diaphragm muscle fibrosis involves changes in collagen organization with mechanical implications in Duchenne muscular dystrophy. Journal of Applied Physiology, 132(3), 653–672. [PubMed: 35050792]

Saini K, Cho S, Dooling LJ, & Discher DE (2020). Tension in fibrils suppresses their enzymatic degradation – A molecular mechanism for ‘use it or lose it.’ Matrix Biology, 85–86, 34–46.

Sanchez GN, Sinha S, Liske H, Chen X, Nguyen V, Delp SL, & Schnitzer MJ (2015). In vivo imaging of human sarcomere twitch dynamics in individual motor units. Neuron, 88(6), 1109–1120. [PubMed: 26687220]

Scarr G. (2016). Fascial hierarchies and the relevance of crossed-helical arrangements of collagen to changes in the shape of muscles. Journal of Bodywork and Movement Therapies, 20(2), 377–387. [PubMed: 27210857]

Smith LR, & Barton ER (2014). Collagen content does not alter the passive mechanical properties of fibrotic skeletal muscle in mdx mice. American Journal of Physiology-Cell Physiology, 306(10), C889–C898. [PubMed: 24598364]

Smith LR, Chambers HG, Subramaniam S, & Lieber RL (2012). Transcriptional abnormalities of hamstring muscle contractures in children with cerebral palsy. PLoS ONE, 7(8), e40686. [PubMed: 22956992]

Smith LR, Lee KS, Ward SR, Chambers HG, & Lieber RL (2011). Hamstring contractures in children with spastic cerebral palsy result from a stiffer extracellular matrix and increased in vivo sarcomere length. The Journal of Physiology, 589(Pt 10), 2625–2639. [PubMed: 21486759]

Smith LR, Pichika R, Meza RC, Gillies AR, Baliki MN, Chambers HG, & Lieber RL (2021). Contribution of extracellular matrix components to the stiffness of skeletal muscle contractures in patients with cerebral palsy. Connective Tissue Research, 62(3), 287–298. [PubMed: 31779492]

Soo B, Howard JJ, Boyd RN, Reid SM, Lanigan A, Wolfe R, Reddihough D, & Graham HK (2006). Hip displacement in cerebral palsy. Journal of Bone and Joint Surgery-American Volume, 88(1), 121–129. [PubMed: 16391257]

Sutherland DH, & Davids JR (1993). Common gait abnormalities of the knee in cerebral palsy. Clinical Orthopaedics and Related Research, (288), 139–147. [PubMed: 8458127]

Ward SR, Tomiya A, Regev GJ, Thacker BE, Benzl RC, Kim CW, & Lieber RL (2009). Passive mechanical properties of the lumbar multifidus muscle support its role as a stabilizer. Journal of Biomechanics, 42(10), 1384–1389. [PubMed: 19457491]

Ward SR, Winters TM, O'Connor SM, & Lieber RL (2020). Non-linear scaling of passive mechanical properties in fibers, bundles, fascicles and whole rabbit muscles. Frontiers in Physiology, 11, 211. [PubMed: 32265730]

Wohlgemuth RP, Feitzinger RM, Henricson KE, Dinh DT, Brashear SE, & Smith LR (2023). The extracellular matrix of dystrophic mouse diaphragm accounts for the majority of its passive stiffness and is resistant to collagenase digestion. Matrix Biology Plus, 18, 100131. [PubMed: 36970609]

Wren TAL, Do KP, Hara R, & Rethlefsen SA (2008). Use of a patella marker to improve tracking of dynamic hip rotation range of motion. Gait & Posture, 27(3), 530–534. [PubMed: 17703941]

Young KW, Kuo BP-P, O'Connor SM, Radic S, & Lieber RL (2017). In vivo sarcomere length measurement in whole muscles during passive stretch and twitch contractions. Biophysical Journal, 112(4), 805–812. [PubMed: 28256239]

Key points

- At matched sarcomere lengths, gracilis muscle mechanics and collagen architecture are similar in TD patients and patients with CP.
- In both TD and CP muscles, collagen fibres dynamically increase their alignment during muscle stretching.
- Aspects of muscle mechanics and collagen architecture are predictive of *in vivo* knee joint motion and radiographic hip displacement in patients with CP.
- Longer sarcomere lengths in CP muscle *in vivo* may alter collagen architecture and biomechanics to drive deficits in joint mobility and gait function.

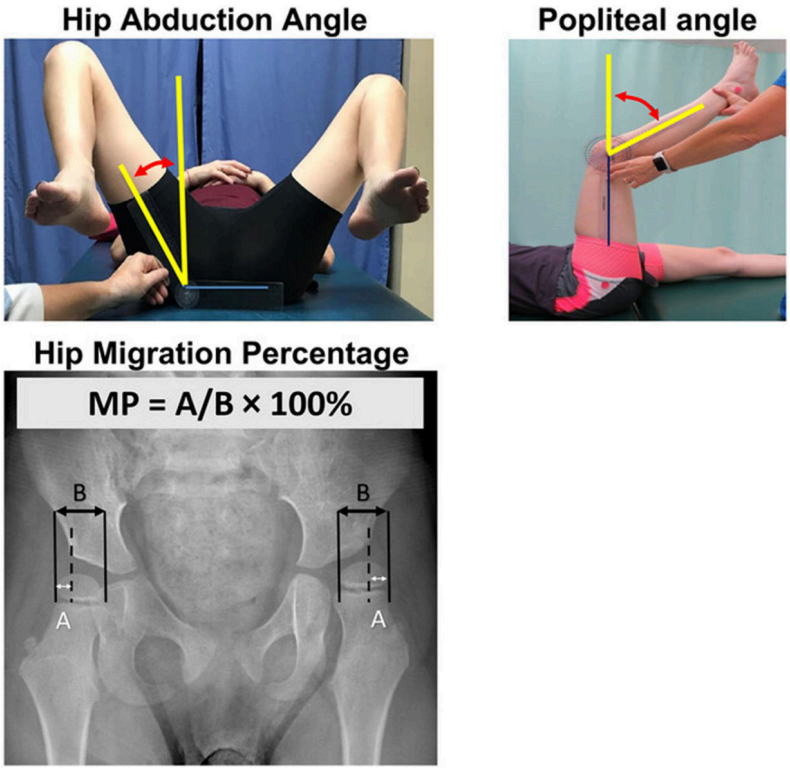

Figure 1. Clinical measures of joint mobility

Hip abduction angle was measured intra-operatively with the sacrum positioned flat on the operating room table and hips flexed to 90°, with each hip's abduction angle measured as the angle between the thigh relative to vertical. Popliteal angles were measured intra-operatively and were defined as the angle of the lower leg relative to vertical during passive knee extension with the hip flexed at 90°. Hip migration percentage (MP), the most important radiographic measure of clinical hip displacement, was calculated from a supine anterior–posterior pelvis radiograph. MP = $A/B \times 100\%$, where A is distance between the lateral edge of the acetabulum to the lateral edge of the femoral head and B is the width of the femoral head.

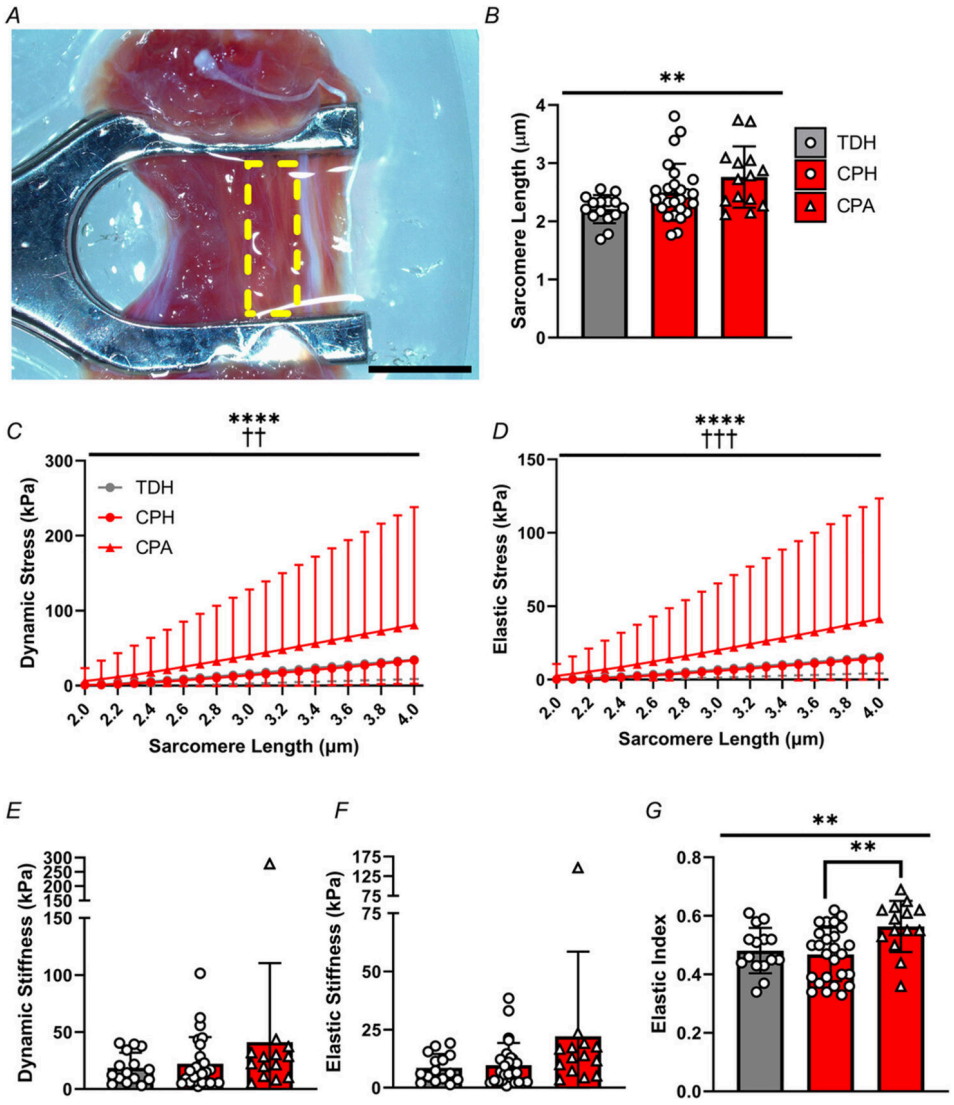

Figure 2. Sarcomere length and passive mechanical properties of muscles from patients with cerebral palsy (CP) or who are typically developing (TD)

A, image of a CP gracilis muscle biopsy clamped at *in vivo* length corresponding to 90° hip and knee flexion. Yellow dashed rectangle indicates a representative site of muscle bundle excision. *B*, clamped sarcomere length was significantly different across muscle groups and tended to be higher in CP muscles. *C* and *D*, there were significant effects of strain and the interaction of strain and muscle group on the dynamic and elastic stress of TDH and CP muscles. *E* and *F*, dynamic and elastic stiffness were not significantly different between muscle groups. *G*, elastic index was higher in CPA muscle bundles compared to CPH. Scale bar is 5 mm. For *B*–*E*, significant main effects and pairwise differences by muscle group: $^{**}P < 0.01$. For *F* and *G*, significant main effect of strain by muscle group: $^{****}P < 0.0001$, significant interaction effect of strain and muscle group: $^{††}P < 0.01$, $^{†††}P < 0.001$.

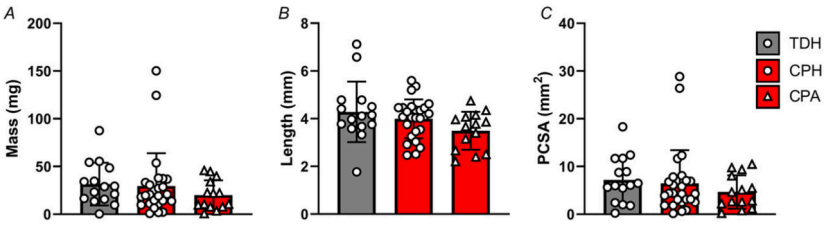

Figure 3. Size characteristics of human muscle biopsies

A–C, there were no significant differences in mass, length and physiological cross-sectional area (PCSA) of muscle biopsies across muscle groups.

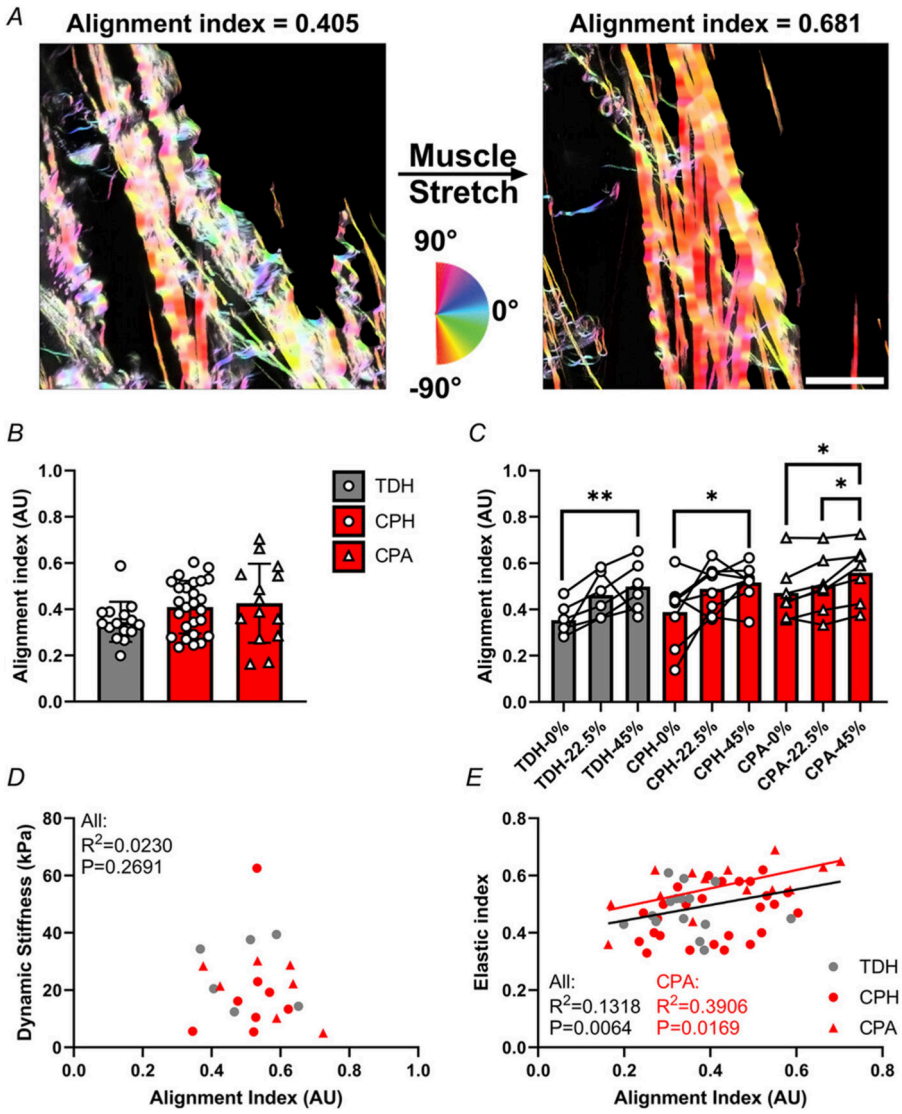

Figure 4. Collagen fibres dynamically increase alignment in response to passive stretching

A, images taken with second harmonic generation microscopy show an increase in collagen alignment with passive muscle stretching. Alignment was calculated using the OrientationJ plug-in in FIJI (Brashear et al., 2021, 2022; Hu et al., 2021). *B*, alignment index of collagen fibres within muscle biopsies at clamped length was not significantly different between TDH and CP muscles. *C*, collagen fibre alignment index significantly increased with strain in TDH and CP muscles. *D*, there was no significant correlation between alignment index and dynamic stiffness at 45% strain. *E*, alignment index at clamped muscle length was positively correlated to elastic index across muscles and within CPA muscles. Scale bar is 100 μm. Significant pairwise differences within muscle groups: $*P < 0.05$, $**P < 0.01$.

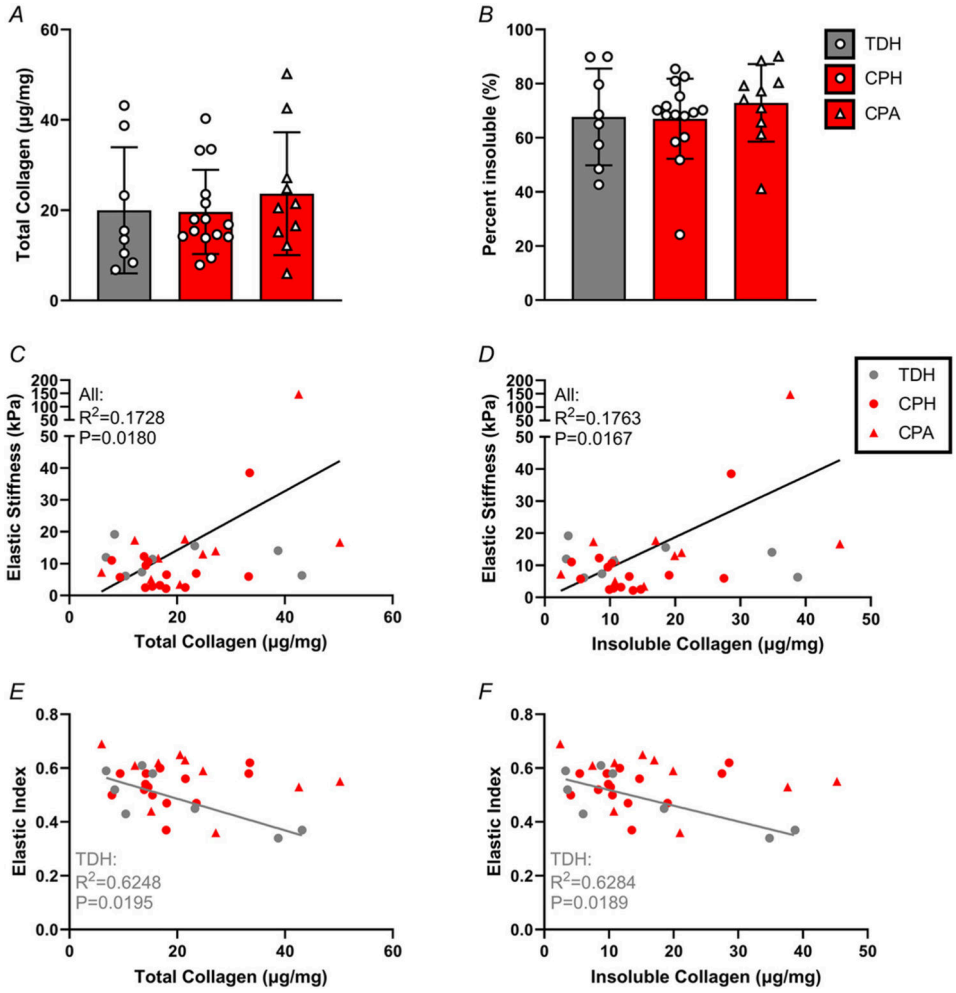

Figure 5. Collagen content and cross-linking are similar between TDH and CP muscles

A and *B*, total and insoluble (cross-linked) collagen contents were not significantly different between muscle groups. *C* and *D*, total and insoluble collagen content positively correlated to elastic stiffness across muscle groups, but not within individual muscles. *E* and *F*, total and insoluble collagen negatively correlated with elastic index in TDH muscles.

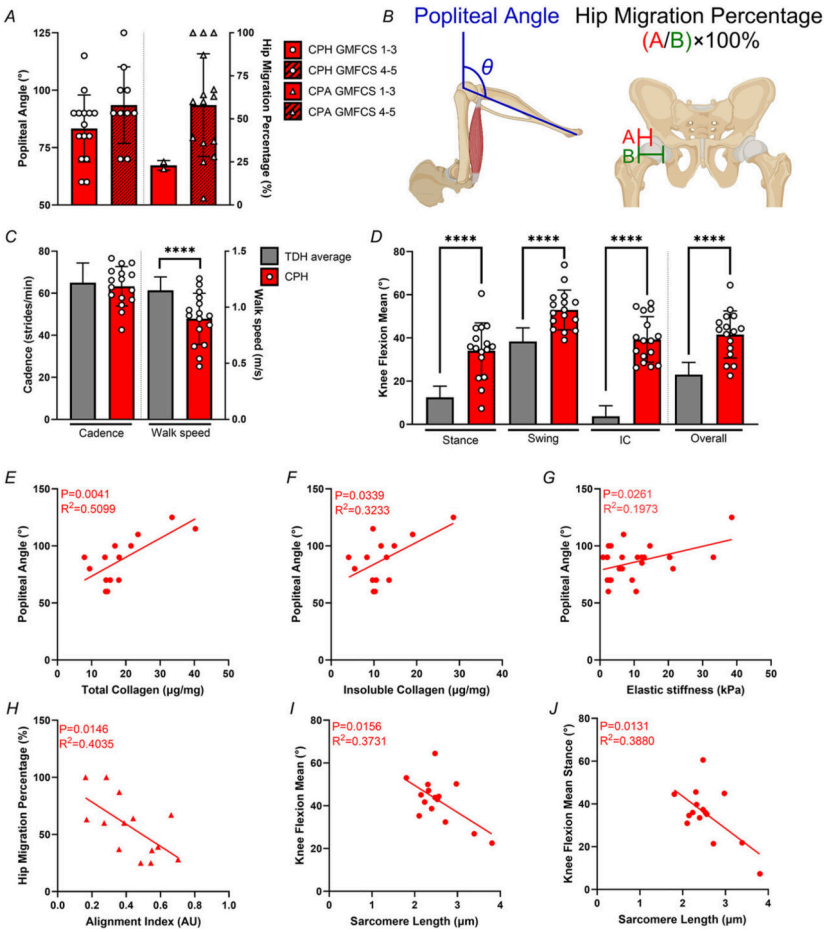

Figure 6. Sarcomere length, collagen architecture and passive muscle mechanics relate to gait and range of motion in patients with CP

A, popliteal angle and hip migration percentage were not significantly different between patients with GMFCS levels 1–3 and GMFCS levels 4–5. *B*, schematic representation of popliteal angle measurement (blue angle) and hip migration percentage calculation (green and red capped lines). Popliteal angle was measured in surgery as the angle above the knee relative to the vertical during passive assisted knee extension. Hip migration percentage was calculated from X-ray images by taking a proportion of the femoral head that is uncovered from the acetabulum. *C*, walk speed was significantly slower in patient with CPH contractures compared to TD patients. *D*, the degree of knee flexion throughout the gait cycle was significantly higher in patients with CPH contractures compared to TD patients. *E–G*, total collagen, insoluble collagen, and elastic muscle stiffness all positively correlated to higher popliteal angle in patients with CPH contractures. *H*, higher collagen alignment index was correlated to reduced hip migration percentage in patients with CPA contractures. *I* and *J*, clamped (*in vivo*) sarcomere length was negatively correlated to the degree of knee flexion across the gait cycle and in the stance phase in patients with CPH contractures. Pairwise differences by muscle group: ****$P < 0.0001$. This figure was produced in part using BioRender.com.

Table 1.

Patient data

Group	*n*	Age	Sex	GMFCS	Popliteal angle	Hip Abduction Angle	Hip Migration Percentage
TDH	15	14.27 ± 1.87	6 M, 9 F	N/A	N/A	N/A	N/A
CPH	27	10.52 ± 3.04	17 M, 10 F	I (2), II (8), III (6), IV (9), V (2)	89 ± 15	N/A	N/A
CPA	14	9.36 ± 4.41	9 M, 5 F	II (1), IV (6), V (7)	N/A	27.27 ± 23.49	57.64 ± 25.61